International Journal of GEOMATE, Nov., 2019 Vol.17, Issue 63, pp. 224- 232
ISSN: 2186-2982 (P), 2186-2990 (O), Japan, DOI: https://doi.org/10.21660/2019.63.92619
Geotechnique, Construction Materials and Environment

# EXPERIMENTAL STUDY ON THE DILATANCY OF ROCK SALT FROM AN UNLOADING PATH

Yunfeng Zhao[1], *Jinyang Fan[1], Deyi Jiang[1], Xiang Jiang[2] and *Wei Liu[1]

[1] State Key Laboratory of the Coal Mine Disaster Dynamics and Controls, Chongqing University, China;
[2] School of Civil Engineering, Chongqing University, China

*Corresponding Author, Received: 03 April 2019, Revised: 24 April 2019, Accepted: 15 May 2019

**ABSTRACT:** As underground storages produce gas, rock salt would always be in unloading paths. The dilatancy behavior of the surrounding rock salt has a great significance for the stability and tightness of the storages. This study investigated dilatancy properties of the rock salt from unloading paths where the confining pressure decreased progressively while the axial pressure was kept fixed. The results showed that: the initial confining pressure value has a rare influence on the dilatancy of the rock salt; an increasing axial pressure can promote the dilatancy of the rock salt; a slower unloading rate and higher temperature would accelerate the dilatancy rate and augment the total volumetric expansion. Compared with the results from conventional loading paths, the compression-dilatancy point is independent of the loading types and remain unchanged in cyclic loading tests. An empirical model to predict compression-dilatancy point was proposed. This model has a certain degree of the engineering significance for designing the operating gas pressure and predicting the dilatancy deformation of the surrounding rock, including porosity variation and permeability.

*Keywords: Rock salt, Dilatancy point, Unloading confining pressure, Dislocation, Temperature*

## 1. INTRODUCTION

In order to respond to the "Paris Agreement" and show China's determination to enforce environmental protection, the Chinese government is trying to change the energy consumption structure by increasing the weight of clean energy, like natural gas, in the primary energy [1,2]. In 2017, China's natural gas import reached 9.2×1010 $m^3$, having a great increase of 27.6%. However, due to the shortage of gas storage facilities, there are frequent gas supply shortages, which bring a lot of inconvenience to people's lives and generate losses for the national economy [3,4].

Underground salt caverns with low permeability and excellent creep performance, is recognized as one of the most effective and stable storage method for natural gas and oil, etc. [5]. Until now, more than 60 salt caverns have been constructed in Europe, with a working gas capacity of more than 500×108 $m^3$. At the end of 2012, there were 40 salt cavern gas storages in America [6]. The Chinese government is attaching more and more important to the underground salt cavern gas storage (UGS) technology, and therefore a large number of UGSs are being constructed.

In terms of a salt cavern, its stability and tightness are essential issues. Dilatancy behavior of the surrounding rock is an appropriate indicator which can simultaneously reflect the stability and permeability change of rock [7-9]. A lot of research shows that a minor dilatancy (< 0.2 vol.%) can lead to a large increase in permeability [10-13]; on the other hand, dilatancy behavior indicates the development of the plastic deformation in rocks and dilatancy angle plays a key role in predicting the failure of rocks [14,15]. Therefore, investigating the dilatancy behavior of the rock salt could give designers and constructors a better understanding of salt cavern surrounding rocks. Hunsche and Hampel [16] proposed an elastoviscoplastic constitutive describing dilatancy, healing, damage, failure, and deformation of rock salt. Moghadam et al [17] improved the elasto-viscoplastic constitutive model and utilized finite element method to simulate the stress variation and ground movement during creep of rock salt around the cavern within the framework of large deformations. Walton and Diederichs [18] established a brittle strength and dilatancy models to predict the stress re-distribution and yield around the shaft. Yang and Jing [19] analyzed the effect of bolt number and joint angle on the deformation and dilatancy behavior of the jointed rock mass. Tan et al [20] used triaxial compression tests and numerically simulated to experimentally observe the permeability evolution during progressive failure of the granite. Alkan et al [21] reported the results of an experimental investigation of the dilatancy behavior and its influence on salt cavern and implied that the main reason for the isolation failure of salt gas storage is the generation and development of the dilatancy in the excavated disturbed zone along the boundary of cavity and rock.

Rock pillars between UGSs are usually the weak spots for salt caverns. Figure 1 illustrates a

representative UGS group, Jintan salt mine, in Jiansu province, China. When a UGS is producing gas, the horizontal stress of the pillar rock and surrounding rock progressively decreases, whereas the vertical pressure almost remains unchanged. The deviatoric stress increase may arise a concomitant dilatancy and induce potential damage to the stability of UGS. When the UGS is in the construction or production stage, the surrounding rock is usually in a state of unloading. However, most of the aforementioned calculating models and methods were based on the conventional loading tests, resulting in limitations of the previous results applied in analyzing the stability and isolation performance of salt cavern.

As the dilatancy behavior of the surrounding rock salt has a great significance regarding the stability and tightness of the storages, this study focused on the dilatancy characteristics of the rock salt from an unloading path to reveal the dilatancy behavior of the surrounding rock salt during the construction or production stage of the UGS.

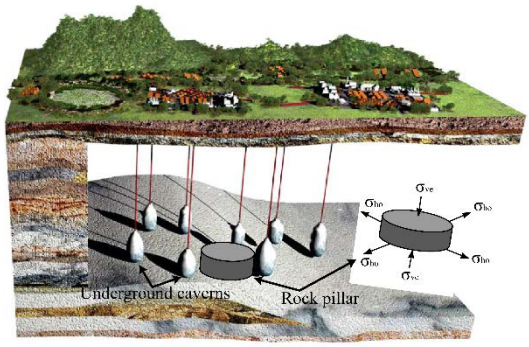


Fig.1 Diagram of the representative underground salt cavern group. $\sigma_{ho}$ is the horizontal stress, $\sigma_{ve}$ is the vertical stress.

## 2. TEST CONDITIONS AND TEST SCHEME

The rock salt samples were collected from the Khewra salt mine, Pakistan and shaped into cylinders with 50 mm diameter ×100 mm length and its components were examined with X-ray diffraction analysis (Table 1). The uniaxial compression strength positions rate and some other parameters were measured with a group of conventional triaxial (including uniaxial) compression tests and shown in Table 2. The unloading experiments were performed on machine MTS815.03 Electro-Hydraulic Servo Rock Experiment System.

Table 1 Components of tested rock salt

| Components | NaCl | $K_2SO_3$ | Mud and others |
|---|---|---|---|
| Percentage composition (%) | 96 | 3.1 | 0.9 |

Table 2 Elastic parameters with different confining pressure

| Confining pressure $\boldsymbol{P_c}$/MPa | 0 | 3 | 5 | 7 |
|---|---|---|---|---|
| Elastic modulus $\boldsymbol{E}$/GPa | 6.50 | 7.40 | 8.10 | 8.65 |
| Possion's ratio $\boldsymbol{\mu}$ | 0.07 | 0.11 | 0.14 | 0.16 |
| Compression strength $\boldsymbol{\sigma_c}$ /MPa | 47.1 | 75.2 | 89.3 | 106 |
| Axial strain corresponding to $\boldsymbol{\sigma_c}$(%) | 8.9 | 19.9 | 25.3 | 29.1 |

The testing procedures: (i) Preparation phase: increase hydrostatically up to a level of the confining pressure, then increase the axial pressure to a value with a loading rate of 0.02 MPa/s. (ii) Unloading phase: hold the axial pressure constant and gradually reduce the confining pressure to 0 by a constant loading rate. Based on the confining pressure, axial pressure, unloading rate and the temperature, 4 groups of experimental tests were designed and listed in Table 3 in detail.

Table 3 Test scheme

| Groups | Axis pressure /MPa | Confining pressure /MPa | Temperature /℃ | Unloading rate /MPa•s$^{-1}$ |
|---|---|---|---|---|
| Temperature group | 25 | 15 | 15,30,45,60 | 0.005 |
| Axis pressure group | 20,25,30,35 | 15 | 22 | 0.005 |
| Confining pressure group | 25 | 10,15,20 | 22 | 0.005 |
| Unloading rate group | 25 | 15 | 22 | 0.005,0.02,0.1,0.5 |

The plastic volumetric strain was calculated as follows:

$$\varepsilon_{ax} = \Delta L/L \quad (1)$$
$$\varepsilon_{la} = \Delta x/(2\pi R) \quad (2)$$
$$\varepsilon_v^p = \varepsilon_{ax} + 2\varepsilon_{la} - \sigma_m/K \quad (3)$$

Where $\Delta L$ is the axial displacement measured by a LVDT device; $L$ is the length of the sample; $\Delta x$ is the elongation of extensometer twining around the sample surface, $R$ is the radius of the sample; $\sigma_m$ is the mean stress. $K$ is the bulk modulus. This is coherent with the results obtained by other scholars [22-24]. The compression-dilatancy point (CDP) is defined when the sample has the minimum value of volume under unloading since after that the sample starts to volumetrically expand.

## 3. RESULTS

### 3.1 CDP in unloading tests

In this work, a positive sign means expansion while a negative sign would represent compression. After the preparation stage, some deformation was produced but was not reckoned in the analysis. All the deformations started from zero. Figure 2 shows representative curves of the volumetric strain *vs* the stress difference $(\sigma_1 - \sigma_3)$ from an unloading test. It can be found that the sample's volume expands once the unloading phase starts. Since the confining pressure was dropping, the bulk stress was decreasing too. It is not unexpected that the volumetric strain goes to positive and increases at the beginning. When the plasticity of the rock salt initiates, dilatancy occurs and the swell of the sample accelerates around one point. CDP is important to estimate the safety risk for UGS [25,26]. To discern where the dilatancy point lays, the curve eliminates the elastic deformation. This was shown in rethe d line (Fig.2), where it can obviously be seen that sample' volume developed through two stages: compression stage in which the volumetric strain gets smaller and dilatancy stage where the development trend reverses. The turning point could be easily recognized as the dilatancy point (the star in Fig.2). In compression tests, the elastic volumetric strain was also eliminated. The dilatancy point was distinguished using the same method, which will be discussed later.

### 3.2 Effect of stress

Confining pressure generally plays a role in preventing the damage, restraining the development of plastic deformation and microcrack prorogating.

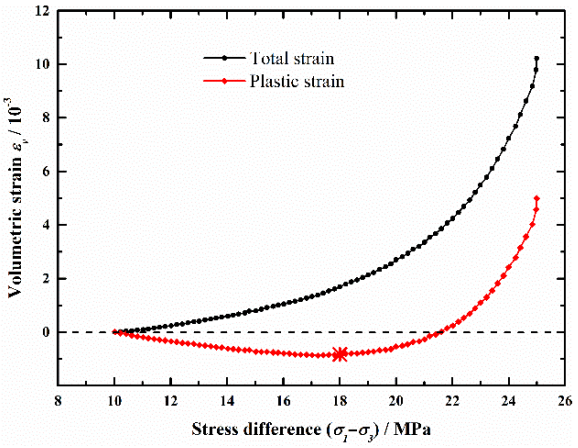


Fig.2 Representative curves of the volumetric strain *vs* the stress difference from axis pressure group test.

This effect had a clear boundary: when the confining pressure was larger than the critical value, dilatancy would be strongly controlled and not occur; in the opposite case, the restrain effect receded and dilatancy was produced. Dilatancy point should be this critical value, which was marked on the curves of the tested samples with different initial confining pressures (Fig.3). The results showed that the initial confining pressure has a rare or inconspicuous influence on the dilatancy point. A smaller initial pressure does not change the dilatancy stage but extends the time of the compression stage and the magnitude of volume shrink in the test.

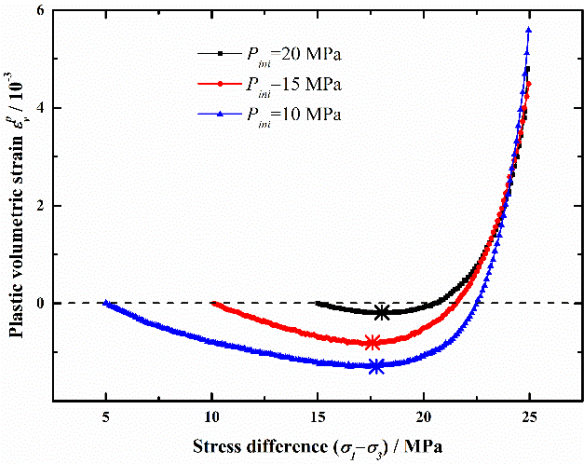


Fig.3 Stress difference *vs* volumetric strain curves of the specimens from confining pressure group. $P_{ini}$ represents the initial confining pressure.

The effect of the axial pressure is different from that of the confining pressure, remarkably changing the dilatancy rate and CDP. Figure 4 shows these

points from the tests under different axial pressures. As the axial pressure increases from 20 MPa to 25 MPa, 30 MPa, and 35 MPa, the critical deviatoric stress (the stress state corresponding to the dilatancy point is called critical stress in this study) changes from 15.78 MPa to 18.11 MPa, 22.08 MPa, 25.04 MPa, respectively. By fitting, it can be seen that the increasing axial pressure give rise to a linear increase in critical stress. Additionally, what is worth noticing is that the strain rate and the deformation amplitude (the difference between a minimum value and end value) in the dilatancy stage also increase with axial pressure.

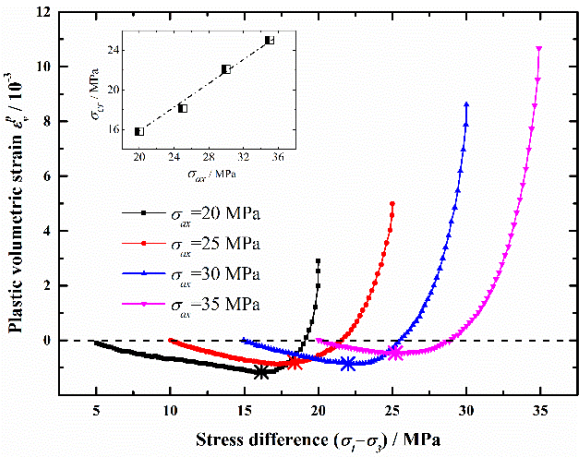


Fig.4 Stress difference *vs* volumetric strain curves of specimens from the axial pressure group. The inset in the top-right corner shows the relationship between axial stress and critical stress. $\sigma_{ax}$ represents the axial pressure. $\sigma_{cr}$ represents the critical stress difference. The critical deviatoric stresses are 15.78, 18.11, 22.08, 25.04 MPa.

### 3.3 Effect of unloading rate and temperature

A stage with ever-changing unloading rate is meaningless for analyzing the effect of unloading rate. An Electro-Hydraulic Servo System will adjust the unloading rate when the target value is judged to be near. After eliminating the inconstant period, Fig.5 shows the curves from the samples with different unloading rates and the same stress state. The influence of the unloading rate on dilatancy properties of the rock salt is mainly reflected in two aspects. (i) Both the amplitude of the dilatancy and the deformation increase with the diminishing unloading rate. (ii) Decreasing unloading rate promotes a smaller critical deviatoric stress.

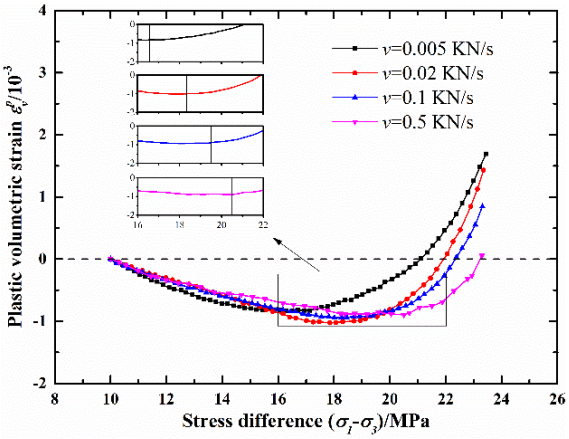


Fig.5 Stress difference *vs* volumetric strain curves of the specimens from unloading rate group. *v* represents the unloading rate. The critical stress differences are 16.58, 18.3, 19.59, 20.5 MPa.

The samples in the temperature group were tested at 15℃, 30℃, 45℃ and 60℃ (curves can be seen in Fig.6) respectively. The effects of temperature on dilatancy properties of the rock salt are: (i) a higher temperature brings a smaller critical deviatoric stress. (ii) As temperature increases, the dilatancy rate and dilatancy amplitude increase.

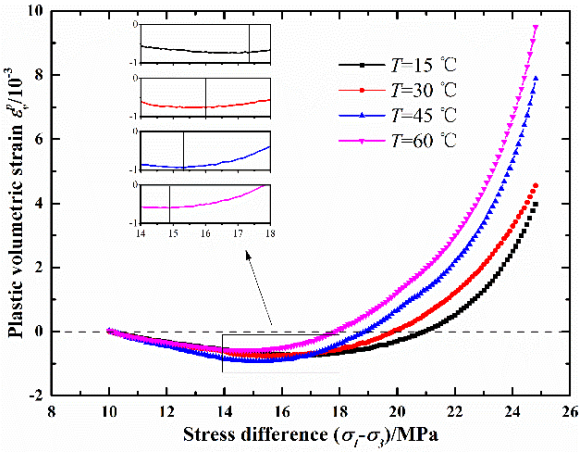


Fig.6 Stress difference *vs* volumetric strain curves of the specimens from temperature group. *T* represents the temperature. The critical stress differences are 17.41, 16.01, 15.31, 14.91 MPa.

## 4. DISCUSSIONS

### 4.1 Mechanism of dilatancy effected by unloading rate and temperature

Rock salt is a kind of crystal material. Its plastic strain is essentially the consequences of crystal dislocations, which induces the dilatancy phenomenon [27,28]. Figure 7 shows a group of

parallel slip lines of dislocations of a sample from an unloading test. Dislocations will move under a stress and pile up when countering obstacles. As the obstructed dislocations are in a certain amount, ruptures/dilatancy will form. The moving velocity of dislocations in the crystal can be estimated by the Eqs. (4) and (5) [29].

$$v = B \times (\sigma_*)^{m*} \quad (4)$$

$$v = v_c \exp(\frac{-\Delta F^{\neq}}{kT}) \quad (5)$$

Where $\sigma^*$ is the effective stress, $m^*$ is the stress sensitivity coefficient, related with absolute temperature $T$. $k$ is the Boltzmann constant, $\Delta F^{\neq}$ is the standard activation energy which is the energy needed to fully activate the dislocation. $v_c$ is the speed when the standard activation energy is zero.

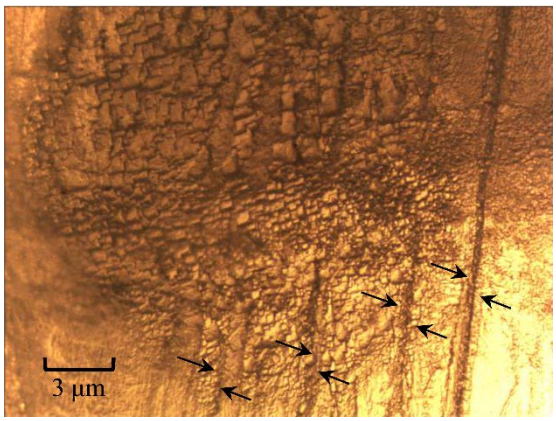


Fig.7 Dislocation slip line observed in the tested salt material.

The mechanism of the stress' effect on dilatancy is understandable, according to the Eq. (2), and will not be reiterated here. Unloading rate influences the dislocation via sliding time. As the stress and temperature are identical in the unloading rate group, there will be less time for dislocations to proliferate and coalesce with predetermined dislocation under a faster unloading rate and as a result, grain dislocations have a lower density. The dilatancy deformation is smaller with a faster unloading rate.

According to Eq. (5), temperature speeds up the movement of dislocations. Moreover, a higher temperature could enhance the thermal motion of atoms, facilitate dislocations proliferation and help dislocations overcome the higher level of barriers [29]. Therefore, a higher temperature induces more dislocation inside the rock salt, promoting a lager dilatancy deformation. The CDP marks the difficulty degree of the dilatancy deformation. A higher temperature represents an easier circumstance for a dislocation to proliferate and slide.

The obtained results suggest that a relatively faster injection or production rate is favorable to UGS, which will cause a smaller dilatancy for the surrounding rock, especially for the rock pillar. Regarding the stress effect, the depth of UGS has a significant influence on the dilatancy, but gas pressure has little. On the other hand, UGS should have minimum deviatoric stress in order to prevent the dilatancy. However, the stress state of a UGS is determined only after its depth and design operation pressure is decided, and therefore is impossible to optionally change. Temperature is an environmental variable. As the depth of UGS grows, the environmental temperature and the axial stress will increase, leading to an inevitable faster dilatancy deformation rate. In a word, UGS should be constructed at a small depth on a promise of stability and tightness. Since the deviatoric stress usually comes to the minimum after injection in summer, the injection rate should be as fast as possible. After autumn, a slower production in winter is suggested.

### 4.2 Critical stress of salt in unloading path

As some scholars assumed [25,26], critical deviatoric stress has a close relationship with axial stress. The inset of Fig.4 shows the curve of the critical deviatoric stress *vs* the axial stress from the axial pressure group. By fitting in Fig.8, the relationship between critical stress and axial stress could be obtained as Eq. (6).

$$\sigma_{cr}(\sigma) = k_1 \sigma_{ax} + b_1 \quad (6)$$

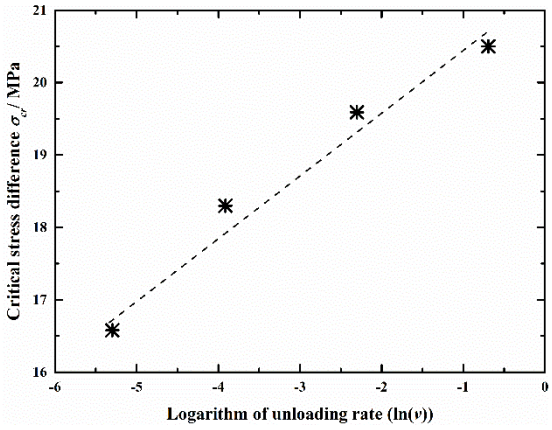


Fig.8 Curve of critical stress difference *vs* logarithm of unloading rate.

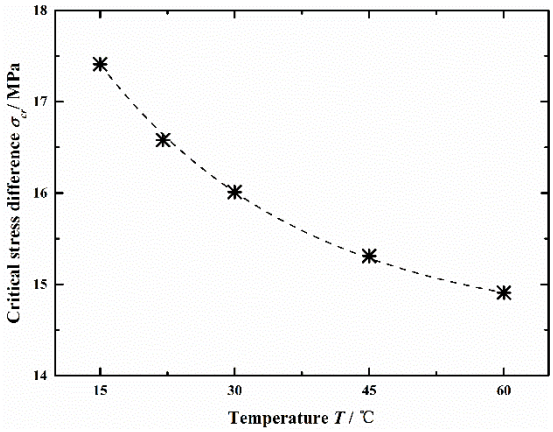


Fig.9 Curve of critical stress difference *vs* temperature.

The relation of the critical stress to the unloading rate and temperature (Fig.8 and Fig.9) could be obtained from the unloading rate group and the temperature group as shown in Eqs. (7) and (8), respectively.

$$\sigma_{cr}(v) = k_2 \ln v + b_2 \quad (7)$$

$$\sigma_{cr}(T) = aT^b \quad (8)$$

With the limited experimental data, the effects of stress, temperature and unloading rate are assumed independent, thus the empirical model of the critical stress is as follow:

$$\sigma_{cr} = K_1\sigma_{ax} + K_2 \ln v + AT^b + d \quad (9)$$

Where $T$ and $v$ are the temperature and the unloading rate, respectively. $K_1$, $K_2$ and $A$ are the stress factor, the unloading rate factor and the temperature factor, representing the factors' weight. $d$ is a baseline value; $b$ is a fitting parameter. $K_1$=1.107, $K_2$=0.841, $A$=23.489, $b$=-0.112, $d$=-5.7.

### 4.3 Critical stress of salt in loading and unloading path

CDPs from loading paths were marked on the curves of conventional compression tests with different confining pressures (Fig.10). A small reduction in the sample volume leads to the microcrack compaction. The critical stress increased as expected with the increasing confining pressure. Comparing the CDPs from loading and unloading, it can be found that CDPs from the two different loading types are almost the same (Fig.11), implying that the CDPs are independent of the loading type. This suggests that the results obtained from conventional compression tests could also be applied in estimating the dilatancy behavior of salt caverns as the basic experimental data.

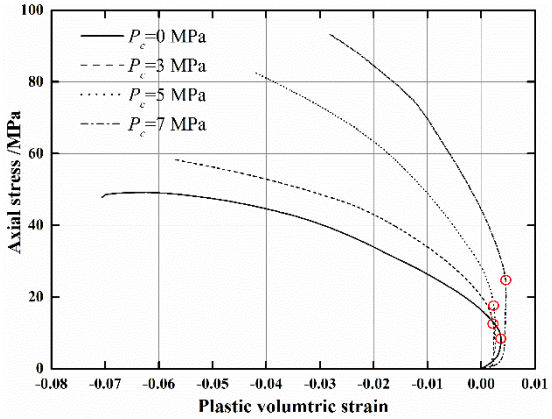


Fig.10 Curves from conventional compression tests with different confining pressure.

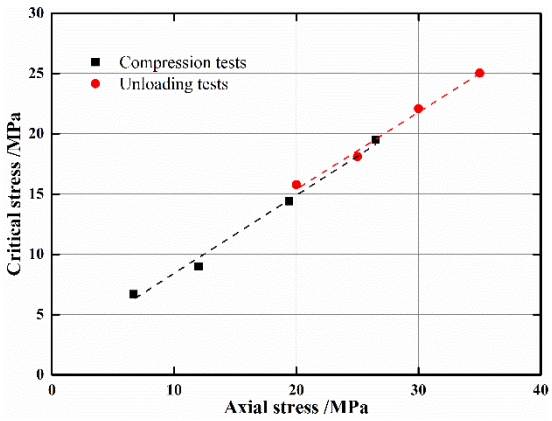


Fig.11 Critical stress *vs* axial stress from conventional compression tests and unloading tests.

A conventional cyclic loading test was conducted to examine the CDP behavior with different damage degree [30,31]. The stress level is assigned with 3%~85% of the compression stress. The loading rate and temperature were the same for the unloading tests. As shown in Fig.12, CDPs in the cycles just fluctuate within a small range, and hardly change until failure. That means the critical stress remains constant as in the first loading. It can be deduced that the CDP of the surrounding rock of UGS remains constant during the operation period.

A helpful suggestion could be that the air/gas pressure inside UGS should remain above the critical stress so as to avoid dilatancy or large plastic deformation. Since CDPs are unchangeable, the basic data can be obtained from typical laboratory compression tests. Then using Eq. (9), the critical stress can be calculated for different depths of UGSs.

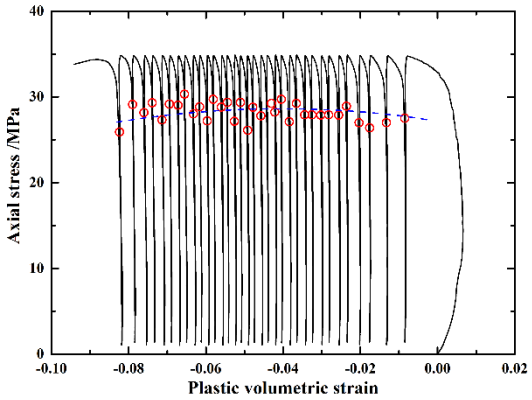


Fig.12 CDPs marked by hollow dots on the curve from cyclic loading tests with a stress level of 3%~85%.

It should be reminded that these experimental laws are obtained within the testing scopes. In China, the universal building depth of salt caverns generally ranges from 600 m to 1800 m. The operation gas pressure ranges from 5 MPa to 18 MPa. Accordingly, the vertical pressure and horizontal pressure of the surrounding rock are in the interval 15-45MPa and 5-20MPa, respectively. Experimental scopes in our unloading tests are able to cover the practical situation acting on the salt cavern. Therefore, the dilatancy model has a certain level of engineering significance in designing the operating gas pressure and predicting the dilatancy deformation of the surrounding rock, including the variation of porosity and permeability by combining the result by Alkan et al [7,21].

## 5. CONCLUSION

In this paper, the rock salt dilatancy properties and mechanism under the action of unloading confining pressure were studied. An empirical dilatancy damage model was also established. Besides, many other observations were made.

I) The initial confining pressure value has a little influence on dilatancy for rock salt. The growth of axial pressure can promote the dilatancy and advance the dilatancy point forward. Meanwhile, the critical deviatoric stress linearly increases with the axial pressure.

II) When undergoing the same stress path, the increasing unloading rate can reduce the dilatancy amplitude, make the dilatancy point shift backward and also decrease the rock salt damage. Regarding dislocation, it was noticed that less time is provided for dislocations to proliferate or coalesce under a faster unloading rate.

III) As the temperature increases, the dilatancy point of the rock salt will move forward, the dilatancy rate will speed up and the dilatancy amplitude will increase. The damage increases as the temperature increases. From the prospect of dislocation, higher temperatures accelerate the movement of dislocations, causing more plastic deformation.

Ⅳ) CDPs are independent of the loading types and remain unchanged in cyclic loading tests. According to the results, it is suggested that UGSs should be constructed at a small depth for ensuring stability and tightness. A fast injection rate and a slower production rate are recommendable. Air/gas pressure inside UGS should remain above the critical stress so as to avoid dilatancy or large plastic deformation.

## 6. ACKNOWLEDGMENTS

This work was supported by the National Natural Science Fund (No. 51834003, 41672292, 51574048), China Postdoctoral Science Foundation (2018M633318), Chongqing Postdoctoral Innovation Program (CQBX201802), the Fundamental Research Funds for the Central Universities (No. 2018CDQYZH0018), which are all greatly appreciated.

## 7. REFERENCES

[1] Khaledi K., Mahmoudi E., Datcheva M., and Schanz T., Analysis of compressed air storage caverns in rock salt considering thermo-mechanical cyclic loading, Environmental Earth Sciences, Vol. 75, Issue 15, 2016, pp.1-17.

[2] Ma H. L., Yang C. H., Li Y. P., Shi X. L., Liu J. F., and Wang T. T., Stability evaluation of the underground gas storage in rock salts based on new partitions of the surrounding rock, Environmental Earth Sciences, Vol. 73, Issue 11, 2015, pp.6911-6925.

[3] Fan J. Y., Liu W., Jiang D. Y., Chen J., Ngaha T., William, Chen J. C., and Daemen J. J. k., Thermodynamic and applicability analysis of a hybrid CAES system using abandoned coal mine in China, Energy, Vol. 157, 2018, pp.31-44.

[4] Yang C. H., Wang T. T., Li J. J., Ma H. L., Shi X. L., and Daemen J. J. K., the Feasibility analysis of using closely spaced caverns in bedded rock salt for underground gas storage: a case study, Environmental Earth Sciences, Vol. 75, Issue 15, 2016.

[5] Mahmoudi E., Khaledi K., Blumenthal A. V., König D., and Schanz T., Concept for an integral approach to explore the behavior of rock salt caverns under thermo-mechanical cyclic loading in energy storage systems, Environmental Earth Sciences, Vol. 75, Issue 14, 2016, pp.1-19.

[6] Zhang Z. P., Zhang R., Xie H. P., Liu J. F., and Were P., Differences in the acoustic emission

characteristics of rock salt compared with granite and marble during the damage evolution process, Environmental Earth Sciences, Vol. 73, Issue 11, 2015, pp.6987-6999.

[7] Alkan H., Percolation model for dilatancy-induced permeability of the excavation damaged zone in rock salt, International Journal of Rock Mechanics and Mining Sciences, Vol. 46, Issue 4, 2009, pp.716-724.

[8] Wan R., Nicot F., and Darve F., Micromechanical Formulation of Stress Dilatancy as a Flow Rule in Plasticity of Granular Materials, Journal of Engineering Mechanics, Vol. 136, Issue 5, 2010, pp.589-598.

[9] Fan J. Y., Jiang D. Y., Liu W., Wu F., Chen J., and Daemen J. J. K. Discontinuous fatigue of salt rock with low-stress intervals, International Journal of Rock Mechanics and Mining Sciences, Vol. 115, Issue 3, 2019, pp.77-86.

[10] Li W. J., Han Y. H., Wang T., and Ma J. W., DEM Micromechanical Modeling and Laboratory Experiment on Creep Behavior of Salt Rock, Journal of Natural Gas Science and Engineering, Vol. 46, 2017, pp.38-46.

[11] Li W. J., Zhu C., Yang C. H., Duan K., and Hu W. R., Experimental and DEM investigations of temperature effect on pure and interbedded rock salt, Journal of Natural Gas Science and Engineering, Vol. 56, 2018, pp.29-41.

[12] Liu W., Muhammad N., Chen J., Spiers C. J., Peach C. J., Jiang D. Y., and Li Y. P., Investigation on the permeability characteristics of bedded salt rocks and the tightness of natural gas caverns in such formations, Journal of Natural Gas Science and Engineering, Vol. 35, 2016, pp. 468-482.

[13] Mahnken R., and Kohlmeier M., Finite element simulation for rock salt with dilatancy boundary coupled to fluid permeation, Computer Methods in Applied Mechanics and Engineering, Vol. 190, Issue 32, 2001, pp.4259-4278.

[14] Alejano L.R., and Alonso E., Considerations of the dilatancy angle in rocks and rock masses, International Journal of Rock Mechanics and Mining Sciences, Vol. 42, Issue 4, 2005, pp.481-507.

[15] Mas D., and Chemenda A. I., Dilatancy factor constrained from the experimental data for rocks and rock-type material, International Journal of Rock Mechanics and Mining Sciences, Vol. 67, Issue 2, 2014, pp.136-144.

[16] Hunsche U., and Hampel A., Rock salt - the mechanical properties of the host rock material for a radioactive waste repository, Engineering Geology, Vol. 52, 1999, pp.271-291.

[17] Moghadam S. N., Nazokkar K., Chalaturnyk R. J., and Mirzabozorg H., Parametric assessment of salt cavern performance using a creep model describing dilatancy and failure, International Journal of Rock Mechanics and Mining Sciences, Vol. 79, 2015, pp.250-267.

[18] Walton G., and Diederichs M. S., A mine shaft case study on the accurate prediction of yield and displacements in the stressed ground using lab-derived material properties, Tunnelling and Underground Space Technology, Vol. 49, 2015, pp.98-113.

[19] Yang S. Q., and Jing H. W., Strength failure and crack coalescence behavior of brittle sandstone samples containing a single fissure under uniaxial compression, International Journal of Fracture, Vol. 168, Issue 2, 2011, pp.227-250.

[20] Tan X., Konietzky H., and Frühwirt T., Experimental and Numerical Study on Evolution of Biot's Coefficient During Failure Process for Brittle Rocks, Rock Mechanics and Rock Engineering, Vol. 48, Issue 3, 2015, pp.1289-1296.

[21] Alkan H., Cinar Y., and Pusch G., Rock salt dilatancy boundary from combined acoustic emission and triaxial compression tests, International Journal of Rock Mechanics and Mining Sciences, Vol. 44, Issue 1, 2007, pp.108-119.

[22] Fuenkajorn K., and Phueakphum D., Effects of cyclic loading on mechanical properties of Maha Sarakham salt, Engineering Geology, Vol. 112, Issue 1, 2010, pp.43-52.

[23] Liang G. C., Huang X., Peng X. Y., Tian Y., and Yu Y. H., Investigation on the cavity evolution of underground salt cavern gas storages, Journal of Natural Gas Science and Engineering, Vol. 33, 2016, pp.118-134.

[24] Ma L. J., Liu X. Y., Wang M. Y., Xu H. F., Hua R. P., Fan P. X., Jiang S. R., Wang G. A., and Yi Q. K., Experimental investigation of the mechanical properties of rock salt under triaxial cyclic loading, International Journal of Rock Mechanics and Mining Sciences, Vol. 62, Issue 9, 2013, pp.34-41.

[25] Mellegard K. D., and Pfeifle T. W., Laboratory evaluation of mechanical properties of rock using an automated triaxial compression test with a constant mean stress criterion, American Society for Testing and Materials, West Conshohocken, PA (US), United States, 1999.

[26] Roberts L. A., Buchholz S. A., Mellegard K. D., and Düsterloh U., Cyclic Loading Effects on the Creep and Dilation of Salt Rock, Rock Mechanics and Rock Engineering, Vol. 48, Issue 6, 2015, pp.2581-2590.

[27] Peach C. J., and Spiers C. J., Influence of crystal plastic deformation on dilatancy and permeability development in synthetic salt rock, Tectonophysics., Vol. 256, Issue 1, 1996, pp.101-128.

[28] Serrano A., Olalla C., and Galindo R. A.,

Micromechanical basis for shear strength of rock discontinuities, International Journal of Rock Mechanics and Mining Sciences, Vol. 70, 2014, pp.33-46.

[29] Zhao J. S., Basis of dislocation theory. National Defense Industry Press, Beijing, 1989.

[30] Fan J. Y., Chen J., Jiang D. Y., Ren S., and Wu J. X., Fatigue properties of rock salt subjected to interval cyclic pressure, International Journal of Fatigue, Vol. 90, Issue 9, 2016, pp.109-115.

[31] Fan J. Y., Chen J., Jiang D. Y., Chemenda A., Chen J. C., and Ambre J., Discontinuous cyclic loading test with acoustic emssion monitoring, International Journal of Fatigue, Vol. 94, Issue 1, 2017, pp.140-144.